

Electrical and Optical Properties of Eu-Doped Indium Oxide Thin Films Deposited by Radio-Frequency Magnetron Sputtering

Jong-Kwan Woo¹ and Shinho Cho^{2,*}

¹Department of Physics, Jeju National University, Jeju 690-756, Republic of Korea

²Department of Materials Science and Engineering, Silla University, Busan 617-736, Republic of Korea

Eu-doped In₂O₃ (EIO) thin films were deposited by radio-frequency magnetron sputtering on glass substrates with varying growth temperatures. All the EIO thin films showed a significant dependence on the growth temperature. From the figure of merit index data, the optimum growth temperature for depositing high-quality EIO thin films was found to be 300 °C. The EIO thin film deposited at 300 °C showed a highly preferential growth orientation along the (222) plane with an average particle size of 160 nm, bandgap energy of 3.94 eV, average optical transmittance of 65.2% in the wavelength range 450–1100 nm, and electrical resistivity of $2.5 \times 10^{-3} \Omega \text{ cm}$. These results indicate that the electrical and optical properties of EIO thin films can be modulated by controlling growth temperature.

Keywords: Thin Film, Sputtering, Growth Temperature.

1. INTRODUCTION

Recently, the doping of rare-earth (RE) ions into wide-bandgap semiconductors such as ZnO, Zn₂TiO₄, and GaN has attracted considerable attention because of its potential applications in the manufacture of solar cells, flat panel displays, transparent conducting electrodes, and optoelectronic devices.^{1–4} The effects of RE ion doping on the electrical and optical properties of In₂O₃ are important for understanding the origin of the optical bandgap and electrical resistivity as well as for the development of electroluminescent materials and devices. In particular, In₂O₃ has several advantages for photonic device applications because of its high optical transparency and electrical conductivity.

Many impurities such as the group III elements Al, Ga, and In or the group V elements P, As, and Sb have been used to improve the electrical and optical properties of wide-bandgap semiconductor films.^{5–7} Among these impurities, trivalent RE elements have a partially filled inner shell shielded from its surroundings by completely filled outer orbitals. Owing to this shielding, the intra 4f-transitions result in very sharp optical emissions at

wavelengths from the ultraviolet to the infrared region.⁸ Therefore, some researchers have used RE elements to incorporate impurities in wide-bandgap semiconductors. Fang et al. prepared transparent conductive Tb-doped ZnO films by radio frequency (rf) reactive magnetron sputtering, and reported that the crystalline quality of ZnO:Tb films increased as the Tb content was increased up to about 4.1%.⁹ Steckl et al. deposited a GaN:RE layer by using solid-source molecular beam epitaxy and a plasma N₂ source. They reported that the visible emission at red, green, and blue wavelengths from GaN doped with Eu, Er, and Tm led to the development of flat panel display devices.⁸ Minami et al. deposited highly transparent and conductive thin films of ZnO doped with a rare-earth element, Sc or Y, by dc magnetron sputtering, and suggested that the optimal doping contents of Sc and Y were approximately 2 and 4 wt%, respectively.¹⁰

In this paper, we report on the effects of the growth temperature on the structural, morphological, optical, and electrical properties of Eu-doped In₂O₃ (EIO) thin films deposited on glass substrates by using an rf magnetron sputtering method. The tuning of the growth temperature may provide a method for the development of high-quality RE-doped In₂O₃ thin films and devices. The optical

*Author to whom correspondence should be addressed.

transmittance and electrical resistivity of the thin films are used to determine the figure of merit index. Furthermore, the variation in the optical bandgap, which is obtained from the Tauc's model and parabolic bands, of EIO thin films is investigated as a function of growth temperature.

2. EXPERIMENTAL DETAILS

EIO thin films were prepared on glass substrates by rf magnetron sputtering using an In_2O_3 target (diameter of 1 inch) mixed with 2 wt% Eu_2O_3 (99.9% purity). The substrates were cleaned in acetone with ultrasonic vibration for 20 min, and then rinsed in methanol and deionized water, and dried by blowing with nitrogen. The EIO powder was synthesized via the solid-state reaction method with In_2O_3 (99.99%) and Eu_2O_3 (99.9%) as the starting materials. Stoichiometric amounts of chemicals were ball-milled with ZrO_2 balls and ethanol at a speed of 300 rpm for 20 h. After being dried in an oven at 40 °C for 20 h and ground using an agate mortar, a batch of the mixture was calcinated at 350 °C for 4 h and sintered at 900 °C for 5 h in a tube-type electric furnace. The mixed powder was pressed under 500 kg/cm² of pressure in air at room temperature into a pellet with a diameter of 1 inch and a thickness of 16 mm.

The chamber was initially evacuated to a pressure on the order of 5×10^{-6} Torr by using a turbo-molecular pump. The working pressure was maintained at 25 mTorr under an Ar gas flow rate of 60 sccm. The distance between the target and substrate was fixed at 50 mm. The target was presputtered for 5 min to clean its surface. The substrate holder was rotated at a rate of 10 rpm, and the deposition was carried out at temperatures of 25, 100, 200, 300, and 400 °C at an rf power of 40 W.

The crystalline structure of the EIO films was investigated by X-ray diffraction (XRD, X'Pert PRO-MPD, PANalytical) with $\text{Cu-K}\alpha$ radiation ($\lambda = 0.15406$ nm). The surface of the EIO films was examined by using a field-emission scanning electron microscope (FE-SEM, S-4800, Hitachi). The optical absorbance spectra were measured in the wavelength range 200–1100 nm with an ultraviolet-visible spectrophotometer (Ultraspec-3300 pro, Amersham). The electrical properties were characterized by the van der Pauw method using the Hall-effect measurement system (HMS-5500, Ekopia).

3. RESULTS AND DISCUSSION

Figure 1 shows the XRD patterns of the EIO thin films deposited on glass substrates at growth temperatures of 25, 100, 200, 300, and 400 °C. It can be seen that the film deposited at 25 °C was amorphous without any significant diffraction peaks. However, the films deposited at temperatures greater than or equal to 100 °C were crystalline. For the EIO film deposited at 100 °C, one intense diffraction peak and four weak peaks are observed: the

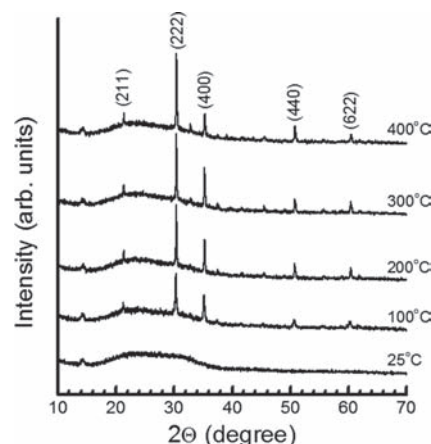


Figure 1. XRD patterns of the EIO thin films deposited at five different growth temperatures.

former occurs at 34.36° with a full width at half-maximum (FWHM) of 0.23°, which corresponds to the diffraction of the In_2O_3 (222) plane; and the latter centered at 21.31°, 35.19°, 50.73°, and 60.19° are identified as the diffractions from the (211), (400), (440), and (622) planes of In_2O_3 , as indicated in JCPDS #76-0152. The observation of preferential growth orientation along the (222) plane is in good agreement with previously reported results.¹¹ The EIO thin films were found to exhibit a body-centered cubic structure. As the growth temperature is increased from 100 to 400 °C, the intensity of the (222) peak increases rapidly, its position moves toward the larger diffraction angle, and the FWHM of the peak shows a decreasing tendency. For the EIO film deposited at 400 °C, the intensity of the (222) diffraction peak is the most intense, and its FWHM is measured to be 0.18°, which indicates an improvement in the crystallinity of the EIO thin film. The average crystallite size of the EIO thin films was determined by using the FWHM and diffraction angle of the (222) main peak and the well-known Scherrer formula.¹² The EIO thin film deposited at 100 °C exhibited a minimum crystallite size of around 40 nm. For films deposited at temperatures greater than 100 °C, the crystallite size shows an overall increasing tendency with growth temperature and reaches a maximum of about 51 nm for the thin film deposited at 400 °C.

Figure 2 shows the SEM surface images of the EIO thin films deposited at five different growth temperatures. For the EIO thin film deposited at 25 °C, very small nanoparticles were developed on top of the glass substrate, as shown in Figure 2(a), but it was extremely difficult to distinguish between the particles and the glass substrate by the naked eye. For the EIO thin film deposited at 100 °C, the surface morphology comprises a large number of cubic-shaped crystalline particles with an average diameter of 40 nm, as shown in Figure 2(b). At growth temperatures of 200 and 300 °C, the grains agglomerate to form larger clusters, and the grain shape changes to cylinder-like particles with an average diameter of 160 nm. The thin film deposited

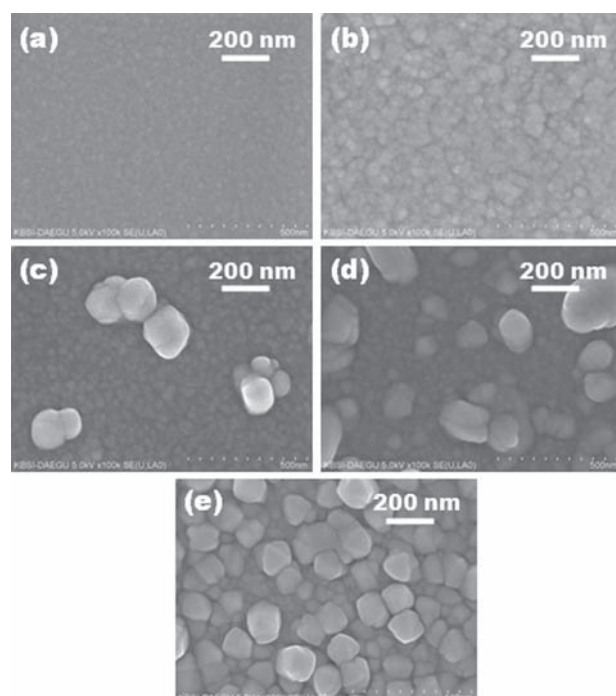


Figure 2. SEM surface images of the EIO thin films deposited at five growth temperatures: (a) 25 °C (b) 100 °C (c) 200 °C (d) 300 °C and (e) 400 °C.

at 400 °C shows a uniform grain-size distribution with a grain size of 110 nm, as shown in Figure 2(e).

Figure 3 shows the optical absorbance and transmittance spectra (inset) for the EIO thin films deposited as a function of growth temperature. The absorption edge for the EIO thin film deposited at 25 °C is at 336 nm. The absorption edge approaches a minimum value of 327 nm

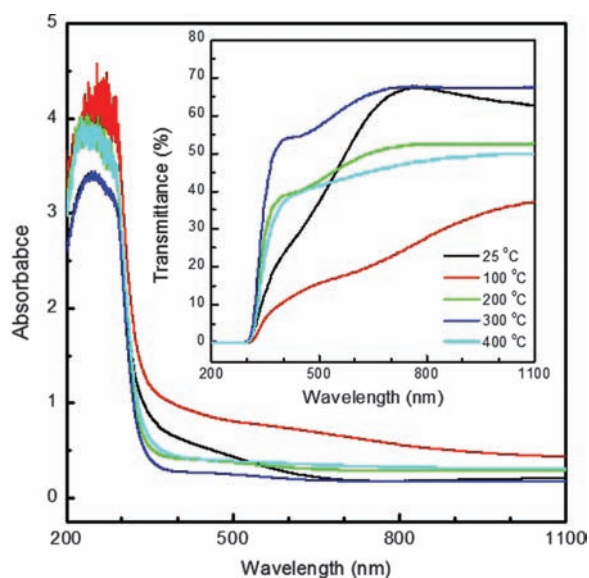


Figure 3. Absorbance and transmittance spectra for the EIO thin films deposited at five different growth temperatures.

at 200 °C. The values of the average transmittance in the wavelength range 450–1100 nm were 59.1, 26.2, 50.2, 65.2, and 46.7% at growth temperatures of 25, 100, 200, 300, and 400 °C, respectively.

Figure 4 shows the optical bandgap energy of the EIO thin films deposited at five different growth temperatures. The bandgap energy can be obtained by extrapolating the line tangential to the horizontal axis in the plot of $(\alpha h\nu)^2$ versus $h\nu$, where $h\nu$ is the photon energy of incident light.¹³ For the EIO thin film deposited at 100 °C, the optical bandgap is found to be 3.80 eV, which is larger than the optical direct bandgap of 3.5–3.7 eV for a pure In_2O_3 thin film at room temperature.¹⁴ As the growth temperature is increased, the optical bandgap of the EIO thin films increases gradually and approaches a maximum value of 3.96 eV at a growth temperature of 200 °C, and then decreases slowly to 3.90 eV at 400 °C, as shown in the inset of Figure 4. A bandgap variation of 160 meV is observed for the two EIO thin films deposited at 100 and 200 °C.

Figure 5 shows the variation in electrical resistivity, Hall mobility, and charge carrier-concentration of the EIO thin films as a function of growth temperature. The EIO thin film grown at 25 °C was found to have a carrier concentration of $2.52 \times 10^{20} \text{ cm}^{-3}$, electrical resistivity of $1.4 \times 10^{-2} \Omega \text{ cm}$, and mobility of $1.75 \text{ cm}^2 \text{ V}^{-1} \text{ s}^{-1}$. The charge-carrier concentration increases gradually with increasing growth temperature, and approaches a maximum value of $3.35 \times 10^{20} \text{ cm}^{-3}$ for the EIO thin film deposited at 100 °C, and then decreases slowly with further increase in growth temperature. In contrast, the electrical resistivity shows an overall decreasing tendency and has a minimum value of $2.5 \times 10^{-3} \Omega \text{ cm}$ for the EIO thin film deposited at 100 °C. This result can be explained by the fact that the

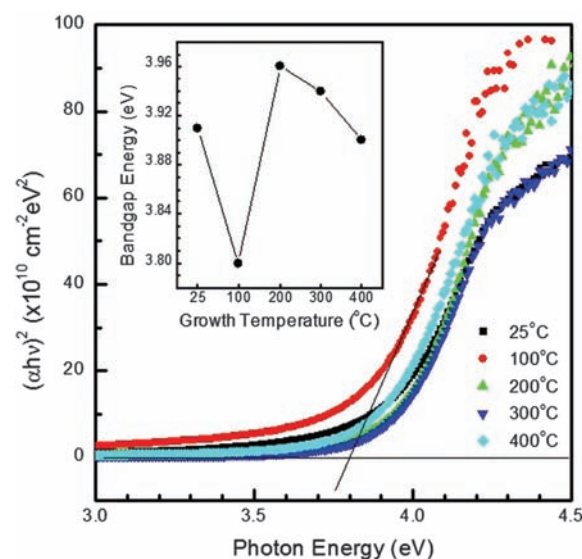


Figure 4. Optical bandgap energy for the EIO thin films deposited at five different temperatures.

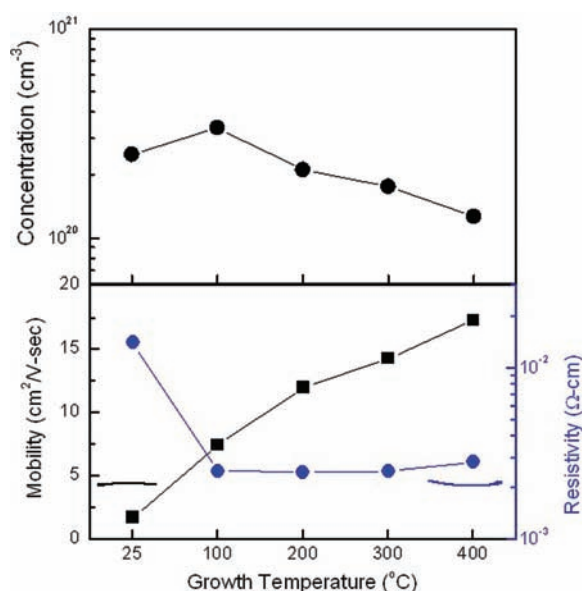


Figure 5. Carrier concentration, mobility, and electrical resistivity of the EIO thin films as a function of growth temperature.

EIO thin film deposited at a growth temperature of 100 °C has the highest carrier concentration, leading to its lower resistivity. All the EIO thin films, irrespective of growth temperature, show *n*-type conduction. The average Hall coefficients of the EIO thin films are found to be -0.025 , -0.019 , -0.029 , -0.036 , and -0.049 cm³/C for the EIO thin films deposited at 25, 100, 200, 300, and 400 °C, respectively. The results confirm that the electrical resistivity is inversely proportional to the carrier concentration.¹⁵

Figure 6 shows the figure of merit of the EIO thin films deposited at five different growth temperatures. The figure of merit F , which is given by the well-known formula

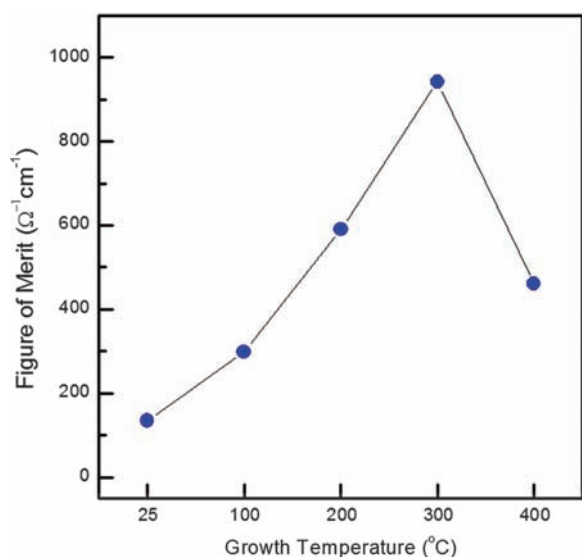


Figure 6. Figure of merit of the EIO thin films deposited at five different growth temperatures.

$F = (-\rho \ln T)^{-1}$, where ρ is the electrical resistivity and T is the average transmittance in the wavelength range 450–1100 nm,¹⁶ can be used for determining the quality of a transparent conducting thin film. For the EIO thin film deposited at 25 °C, the figure of merit was calculated to be $134 \Omega^{-1} \text{ cm}^{-1}$. As the growth temperature increases to 300 °C, the figure of merit increases gradually, reaches a maximum value of $942 \Omega^{-1} \text{ cm}^{-1}$ at a growth temperature of 300 °C, and then decreases rapidly at 400 °C. The significant increase in the figure of merit in the temperature range of 25–300 °C is due mainly to the increase in the transmittance and the decrease in the charge-carrier concentration with increasing growth temperature. The results suggest that the optimum growth temperature for depositing high-quality EIO thin films is 300 °C.

4. CONCLUSION

EIO thin films were deposited on glass substrates by rf magnetron sputtering using a In₂O₃ target mixed with 2 wt% Eu₂O₃ at different growth temperatures from 25 to 400 °C. The XRD data showed that all the EIO thin films except the film deposited at 25 °C showed preferential growth orientation along the (222) plane. Crystalline particles with an average diameter of 110 nm for the thin film deposited at 400 °C were viewed in the FE-SEM image of the substrate surface. An average transmittance of 65.2% for the EIO film deposited at 300 °C was observed in the wavelength range 450–1100 nm. The decrease in electrical resistivity was due mainly to the increase in carrier concentration. The figure of merit for the film deposited at 300 °C was increased seven times compared with that of the thin film grown at 25 °C. The results suggest that the growth temperature plays a key role in controlling the properties of the EIO thin films.

Acknowledgments: This study was supported by Basic Science Research Program through the National Research Foundation of Korea (NRF) funded by the Ministry of Education, Science and Technology (Grant No. 2012010271). The author acknowledges the Korea Basic Science Institute, Daegu branch, for utilizing its FE-SEM facility.

References and Notes

1. S. J. Mrazek, L. Spanhel, M. Surynek, M. Potel, and V. Matejec, *J. Alloys Compd.* 509, 4018 (2011).
2. M. Ungureanu, H. Schmidt, Q. Xu, H. Wenckstern, D. Spemann, H. Hochmuth, M. Lorenz, and M. Grundmann, *Superlattice. Microst.* 42, 231 (2007).
3. X. Gu, L. Zhu, Z. Ye, H. He, and B. Zhao, *Rare Metals* 25, 30 (2006).
4. M. Anbia and S. E. M. Fard, *J. Rare Earth* 30, 38 (2012).
5. J. X. Zhao, X. H. Lu, Y. Z. Zheng, S. Q. Bi, X. Tao, J. F. Chen, and W. Zhou, *Electrochem. Commun.* 32, 14 (2013).
6. S. Y. Lee, *Trans. Electr. Electron. Mater.* 14, 148 (2013).
7. S. H. Jeong, B. N. Park, D. G. Yoo, J. H. Boo, and D. Jung, *J. Korean Phy. Soc.* 50, 622 (2007).

8. A. J. Steckl, J. C. Heikenfeld, D. S. Lee, M. J. Garter, C. C. Baker, Y. Wang, and R. Jones, *IEEE J. Sel. Top. Quant.* 8, 749 (2002).
9. Z. B. Fang, Y. S. Tan, H. X. Gong, C. M. Zhen, Z. W. He, and Y. Y. Wang, *Mater. Lett.* 59, 2611 (2005).
10. T. Minami, T. Yamamoto, and T. Miyata, *Thin Solid Films* 366, 63 (2000).
11. M. Girtan and G. Folcher, *Surf. Coat. Tech.* 172, 242 (2003).
12. S. Cho, *Curr. Appl. Phys.* 10, S443 (2010).
13. M. K. Jayaraj, A. Antony, and M. Ramachandran, *Bull. Mater. Sci.* 25, 227 (2002).
14. D. Beena, K. J. Lethy, R. Vinodkumar, A. P. Detty, V. P. Mahadevanpillai, and V. Ganesan, *Optoelectron. Adv. Mat.* 5, 1 (2011).
15. S. S. Lin, J. L. Huang, and P. Sajgalik, *Surf. Coat. Tech.* 190, 39 (2005).
16. V. Senthilkumar and P. Vickraman, *Curr. Appl. Phys.* 10, 880 (2010).

Received: 10 July 2013. Accepted: 18 March 2014.

Delivered by Publishing Technology to: Universiteit Utrecht
IP: 117.253.106.96 On: Sun, 27 Mar 2016 05:20:37
Copyright: American Scientific Publishers